# Alignment procedure of the LHCb Vertex Detector

S. Viret [a], C. Parkes [a], M. Gersabeck [a]

[a] *Department of Physics and Astronomy, University of Glasgow*
*University Avenue, Glasgow, G12 8QQ, United Kingdom*

**Abstract**

LHCb is one of the four main experiments of the Large Hadron Collider (LHC) project, which will start at CERN in 2008. The experiment is primarily dedicated to B-Physics and hence requires precise vertex reconstruction. The silicon vertex locator (VELO) has a single hit precision of better than 10 $\mu$m and is used both off-line and in the trigger. These requirements place strict constraints on its alignment. Additional challenges for the alignment arise from the detector being retracted between each fill of the LHC and from its unique circular disc r/$\phi$ strip geometry. This paper describes the track based software alignment procedure developed for the VELO. The procedure is primarily based on a non-iterative method using a matrix inversion technique. The procedure is demonstrated with simulated events to be fast, robust and to achieve a suitable alignment precision.

*Key words:* LHCb; Alignment; Vertex Detector;

## 1 Introduction

LHCb is the dedicated heavy flavour physics experiment at the LHC. The physics goals are critically dependent on the performance of the precision vertex locator (VELO). Whilst the intrinsic VELO sensor single hit resolution is $5-10$ $\mu$m for all tracks in the acceptance, the sensors also have to be retracted by 3 cm from the unstable LHC beams while the machine is filled. As a result of these circumstances and the unique geometry of the detector, described in Section 2, the VELO has particularly demanding alignment requirements.

The VELO detector has been assembled with a high precision and a detailed metrology has been performed. However, the only possible method for correcting misalignments during data taking is through a track-based software align-

ment procedure. A new alignment will be performed after each re-insertion of the VELO, in order to check the alignment and ensure optimal data taking.

The alignment procedure is based on techniques which are widely used in particle physics, a comprehensive review of particle physics alignment methods is available in Ref. (1). Two types of techniques are applied here, one is based on matrix inversion and the other on the fitting of functional forms to residual distributions. The LHCb VELO alignment is however unique due to the module and detector geometry and the frequent mechanical retraction of the detector.

The VELO alignment algorithm is divided into three phases: the relative alignment of the sensors in each module; the relative alignment of the modules in each half of the detector; and the relative alignment of the detector-halves. The algorithms are described in Section 3. The results obtained using simulated events are described in Section 4. A summary and conclusions are given in Section 5.

The performance of the first two phases of the alignment procedure were also tested on data during a VELO beam test. The results of this study are presented in Ref. (2) and verify the simulation results presented here.

## 2 The VELO Alignment Context

The VELO consists of two retractable halves, each with 21 modules, as shown in Fig. 1. Each module contains two semi-circular silicon strip sensors that measure r (radial) and $\phi$ (azimuthal angle) co-ordinates, respectively. The strips on the $\phi$ measuring sensor have a stereo angle off-set. A hole up to a radius of 7 mm in the centre of the sensors allows the two proton beams to pass through the VELO, with their interaction point being close to the start of the detector.

The VELO sensors are operated in vacuum and separated from the primary beam vacuum of the LHC by a thin (250 $\mu$m) aluminium foil. The two halves of the VELO will be retracted by 3 cm during each LHC fill until stable beam conditions have been established. Further details of the VELO detector design can be found in Ref. (3).

No magnetic field is applied in the VELO active area, and the residual effects of the LHCb dipole magnet are small. Thus the tracks reconstructed in the detector can be represented by straight lines in the VELO at first order. The effect on the alignment of using straight lines, and hence neglecting the magnetic field and multiple scattering effects, in the VELO have been studied in

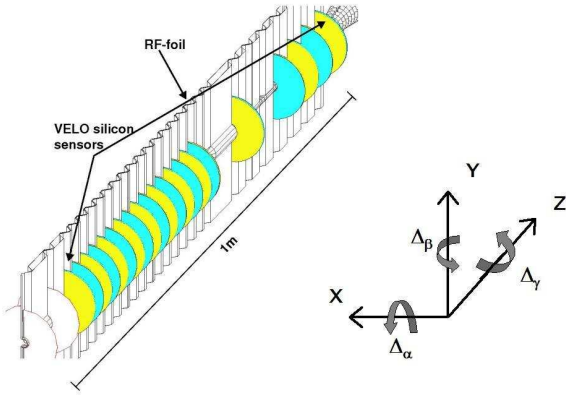


Fig. 1. Layout of the modules in the LHCb vertex detector (left). The right figure describes, in the VELO reference frame, the rotational degrees of freedom used throughout this paper. Rotations around the different axis are applied in the following order: Z ($\Delta_\gamma$), Y' ($\Delta_\beta$), and X" ($\Delta_\alpha$).

simulation. Magnetic field effects could affect the alignment result only when a low momentum track sample with a large charge asymmetry is used. Those effects may be neglected when they are minimized by using an equal number of positively and negatively charged particles. Furthermore, one can use the LHCb Trigger Tracker (4) information (also in an un-aligned environment) to select a track sample with equal numbers for both charges.

The successful operation of the LHCb trigger puts tight constraints on the VELO assembly precision. The LHCb trigger system relies on vertexing but, for speed reasons, the VELO pattern recognition algorithm has to be performed initially in the $r$-z projection. This requires that the strips on the R sensors accurately describe circles around the beam position.

Moreover, remaining misalignments that are not corrected for in software could have significant effects on the trigger performance. For example, a rotation of 0.5 mrad around the Y-axis of one detector can reduce the trigger efficiency by 30 % for the $B_s \to K^+K^-$ channel (5).

## 3 The VELO Alignment Procedure

The alignment of the LHCb VELO proceeds in a number of stages: precision assembly; metrology; and the software alignment described in this paper.

A survey of the VELO system has been performed. The relative position of the $R$ and $\Phi$ sensors on a single module have been measured to an accuracy better than 5 $\mu$m, and no significant curvature of the sensors was observed. The relative position of the VELO modules on the VELO half bases has also been

determined with a similar precision. The survey is of particular importance for determining degrees of freedom that can be constrained less well from tracks, such as the relative z-positions of the VELO modules. Moreover, the survey values have been taken as the initial VELO alignment conditions: the software alignment will be seeded with these values.

The VELO software alignment procedure is divided into three phases. These phases are motivated by and reflect the mechanical construction of the system and the different time periods on which re-alignment is anticipated.

- The first phase performs a relative alignment of $R$ and $\Phi$ sensors within one VELO module (6). The $R$ and $\Phi$ sensors are glued together onto the same hybrid, thus making their relative alignment highly stable. It is anticipated that the alignment of this structure will not need to be repeated as frequently as for the other phases. The alignment technique is based on an iterative fit of the distribution of track residuals across the surface of the silicon sensor.
- The second phase is an internal alignment of the modules within each VELO detector-half (7). The two VELO detector halves are mechanically separate and can be retracted, partially inserted or fully inserted. The VELO halves will be retracted each fill and hence, at least as a cross-check for relative module movement, the alignment will be performed each fill. The alignment technique is based on track residuals applying a non-iterative method using a matrix inversion technique.
- The third phase is the relative alignment of the two halves with respect to each other (8). This will be performed each fill to cross-check and improve upon information provided from the mechanical insertion system. The alignment technique uses the same technique as the module alignment but requiring tracks that pass through both VELO halves and on a similar technique that is applied with vertex constraints.

These three alignment algorithm phases are described in more detail in the following sections.

### *3.1 Relative Sensor Alignment*

A VELO module contains an $R$ and a $\Phi$ sensor glued onto the same hybrid, so that the sensors are back-to-back. The first step of the alignment procedure is to determine the relative alignment of the $R$ and $\Phi$ sensors. This relative alignment is already known to high accuracy from a mechanical survey but can be further improved by applying the following procedure to determine the critical relative x and y translations of the sensors.

As the $R$ and $\Phi$ sensors on each module have to be treated separately, the

residuals with respect to strip hits have to be considered. The unique VELO $R/\Phi$ sensor geometry means that the linearized non-iterative approach applied to space-points in the subsequent alignment phases is not applicable. Instead, an iterative alignment procedure that fits the distribution of residuals as a function of the sensor azimuthal angle has been developed. This procedure is partly inspired by the method developed for the SLD vertex detector (9).

The observed signals on sensor strips are used to determine the best estimate of the hit position. The hits on the sensors (other than those in the module under study) are fitted to produce tracks. These tracks are extrapolated to obtain the track intercept point in the sensor under study. The unbiased residual is then defined as the perpendicular distance between the track intercept point and the line parallel to the strip at the observed hit position. Consequently, these residuals are sensitive to sensor misalignments perpendicular to the strip direction. Since the direction of the strips changes as a function of the azimuthal angle the residuals thus have a well defined sensitivity to translational misalignments in x and y (see Fig. 2).

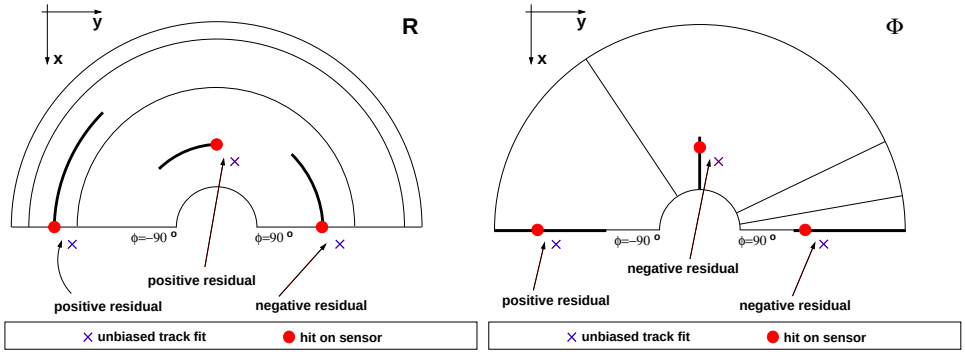


Fig. 2. Influence of misalignments on residuals of $R$ and $\Phi$ sensors. The misalignment shown is a translation both along the negative x and y direction.

It can easily be shown that the relation between residuals ($\epsilon_{R/\Phi}$) and misalignments in the sensor plane ($\Delta_{\mathrm{x}}, \Delta_{\mathrm{y}}, \Delta_{\gamma}$) is given by

$$\begin{cases} \epsilon_R = -\Delta_{\mathrm{x}} \cos\phi_{track} + \Delta_{\mathrm{y}} \sin\phi_{track} & (R \text{ sensor}) \\ \epsilon_\Phi = +\Delta_{\mathrm{x}} \sin\phi_{track} + \Delta_{\mathrm{y}} \cos\phi_{track} + \Delta_{\gamma} r_{track} & (\Phi \text{ sensor}) \end{cases}, \tag{1}$$

where $\phi_{track}$ is the azimuthal angle of the extrapolated track position. $\Delta_\gamma$ describes a misalignment in the form of a rotation around the $z$ axis, which translates into a shift in $\phi$ by multiplication with the radial co-ordinate of the extrapolated track in the sensor plane. As this does not contain any $\phi$ dependence it is sufficient to leave it as a free parameter in the fit.

In practice the alignment constants are determined by an iterative fitting algorithm. For each iteration, the unbiased residuals for the $R$ and $\Phi$ sensor

are plotted against the azimuthal angle. The misalignments are determined through a fit to a binned distribution of the mean residual values as function of $\phi$.

An additional complication arises from the fact that the strips on the VELO $\Phi$ sensors are not exact radial lines. The $\Phi$ sensors are divided into an inner and an outer region within which the strips are tilted through a stereo angle of $20^\circ$ (inner) and $-10.35^\circ$ (outer). This can be compensated for by making the replacement in Eq. 1

$$\phi \rightarrow \phi' = \phi_{min} + \beta,$$

where $\beta$ is the stereo angle and $\phi_{min}$ is the $\phi$ coordinate at the minimal radius of the strip. In addition to preserving the simple relation between the residuals and the alignment constants, this transformation also allows the fit to be made to data from the inner and outer region of the $\Phi$ sensor simultaneously.

This method is primarily used to determine the relative x and y translations of the sensors in a module. However, to improve the fit convergence, the value for $\Delta_\gamma$, the rotation around the $z$-axis of the $\Phi$ sensor, is also determined. This is done using an equivalent approach as above, however now exploiting the distribution of residuals as a function of the track radial co-ordinate. The value for $\Delta_\gamma$ is then determined as the slope of fit with a linear function. However, this relative z rotation of the modules will be extracted to a higher precision using the technique described below in step two of the alignment procedure.

The fitted tracks used in the procedure rely upon the current estimate of the alignment constants of the sensors. Hence it is necessary to iterate this procedure, updating the fitted tracks as the alignment constants are improved.

As the unbiased residuals are determined from a track fitted while excluding hits on both sensors under study, the influence of module to module misalignments vanishes to first order when determining the relative translational misalignment of the sensors. The only misalignments that cannot be determined with this method are common sensor to sensor misalignments of all modules, and sensor to sensor misalignments that have a linear dependency on $z$.

The results of applying this first step of the alignment procedure to simulation events are given in section 4.1.

The second step of the alignment procedure is to perform the relative alignment of the 21 VELO modules within one detector-half. This is based on a non-iterative method using a matrix inversion technique to minimize a $\chi^2$ function.

The $\chi^2$ is produced from the residuals between the tracks and the measured clusters. The measured residuals are expressed as a linear combination of the track parameters and the alignment constants. Each straight line track has four parameters (two slopes and two intercepts) denoted $n_{local}$. The total number of translational and rotational degrees of freedom of all of the modules is $n_{global}$ alignment constants. The track fitting and alignment problem can then be expressed as a system of $n_{total}$ equations, where $n_{total}$ is given by

$$n_{total} \;=\; n_{local} \cdot n_{tracks} \;+\; n_{global}.$$

Clearly, the size of the system scales with the number of tracks used in the alignment. As discussed later, about 20,000 tracks are necessary to obtain a detector-half alignment of the required accuracy. Hence, this implies solving a system of over 80,000 equations, which is a computationally challenging task. However, this problem can be reduced to the size of $n_{global}$ (around 100 for the VELO) using the technique of matrix inversion by partition, performed by the program Millepede[1] (10). This algorithm has already been successfully used in many particle physics experiments (see for example (11; 12))

As stated previously, VELO $R$-sensor strips are semi-circular, thus making $R$-sensor hit information non-linear. However, in order to use the Millepede approach it is mandatory to establish a linear relation between the hit residuals and the misalignments. Here, this is obtained by producing space-points at the VELO module level as described below. This is the natural choice for the VELO as a module containing an $R$ and a $\Phi$ sensor is a independent mechanical object whose internal alignment is expected to be relatively stable.

A particle passing through a VELO module (which is assumed to have its $R$ and $\Phi$ sensors already internally aligned) gives a non-linear set of coordinates: $(r, \mathrm{z}(R_{sensor}))$ and $(\phi, \mathrm{z}(\Phi_{sensor}))$. This system is transformed into an $(\mathrm{x}, \mathrm{y}, \mathrm{z})$ space-point by projecting the $\phi$ information onto the $R$ sensor. As the $\phi$ coordinate of the particle can change slightly in the gap between the $R$ sensor and the $\Phi$ sensor, a correction based on the currently estimated track slopes is applied. Since the correction is small, and the track slope estimates are

[1] a `C++` translation of the `FORTRAN` Millepede program has been implemented by one of the authors of this paper (7).

not significantly biased by the expected module misalignments, the non-linear effects introduced by this procedure are negligible.

An $(r, \phi)$ cluster pair is thus transformed into an (x, y, z) space-point as follows:

$$\begin{cases} \mathrm{x} = r \cdot \cos(\phi_{corr}) \\ \mathrm{y} = r \cdot \sin(\phi_{corr}) \\ \mathrm{z} = \mathrm{z}(R_{sensor}) \end{cases}$$

with

$$\phi_{corr} = \phi + \phi_{track}(R_{sensor}) - \phi_{track}(\Phi_{sensor}).$$

The linear relation between the residuals and the alignment parameters for the VELO modules, which is derived in Ref. (7), is given by:

$$\begin{cases} \epsilon_{\mathrm{x}} = -\Delta_{\mathrm{x}} + \mathrm{y} \cdot \Delta_{\gamma} + a \cdot (\Delta_{\mathrm{z}} + \mathrm{x} \cdot \Delta_{\beta} + \mathrm{y} \cdot \Delta_{\alpha}) \\ \epsilon_{\mathrm{y}} = -\Delta_{\mathrm{y}} - \mathrm{x} \cdot \Delta_{\gamma} + c \cdot (\Delta_{\mathrm{z}} + \mathrm{x} \cdot \Delta_{\beta} + \mathrm{y} \cdot \Delta_{\alpha}) \end{cases} \tag{2}$$

where x, y, z represents the measurement values, and $a$, $c$ are the slopes in the XZ, YZ planes respectively of the track considered. The Millepede technique is then used to simultaneously extract the alignment constants ($\Delta_{\mathrm{x}},\ \Delta_{\mathrm{y}},\ \Delta_{\mathrm{z}},\ \Delta_{\alpha},\ \Delta_{\beta}$ and $\Delta_{\gamma}$) of each of the 21 VELO modules.

An important component of the alignment procedure is the selection of the track sample used. In order to ensure an optimal population of the final matrix, a mixture of tracks coming from the primary interaction point and a complementary set of tracks from the beam halo or beam-gas interactions will be used. A specific pattern recognition algorithm has been developed in order to select these events (13).

The 'weak-modes', *i.e.* deformations which are difficult — if not impossible — to unfold with tracks, are extensively constrained. Two categories of 'weak-modes' have been considered.

Firstly, track residuals are insensitive to linear transformations of the whole detector-half (*e.g.* translation along an axis, or rotation around an axis). The different possible effects are illustrated pictorially in Fig. 3. In three dimensions, this leads to 12 possible global deformations. However, due to the structure of the VELO, we can neglect three of them at first order: shearing in the XY plane, and scaling of the X and Y axes. In addition, due to the VELO geometry, it will be difficult to distinguish XZ and YZ shearings from Y and X rotations. We choose to constrain only the XZ and YZ shearings, as they are easier to add into our linear system.

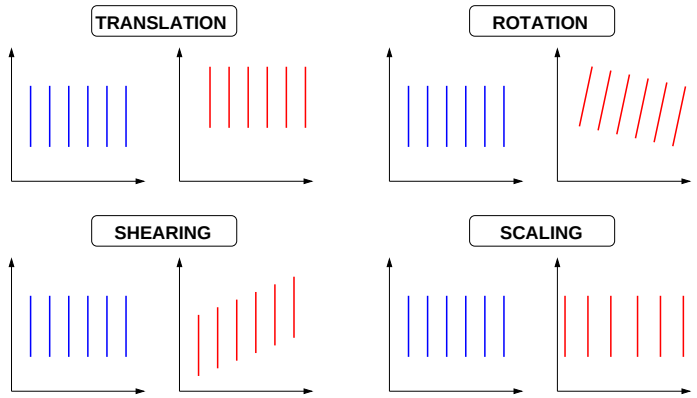


Fig. 3. Linear deformations impossible to constrain via VELO module alignment.

Hence we constrain 7 possible deformations: Z axis rotation, X, Y, Z translations, XZ and YZ shearings, and Z axis scaling. These degrees of freedom are fixed in order to prevent these movements occurring during the module alignment. Within the Millepede framework, this is achieved through Lagrange multipliers, *i.e.* through the addition of constraint equations to the global system.

The second class of 'weak modes' are those that do affect the track residuals but to which there is greatly reduced sensitivity. This is, for example, the case for module rotations around the X-axis, or around the Z-axis with an angle proportional to Z. Even with the best possible track sample the effect on the $\chi^2$ of these modes is comparatively weak, hence they are also weakly constrained by any alignment procedure. Using the survey information as a starting point for the alignment will provide a strong constraint against those special modes. In addition to that, and in order to avoid non-physical variations during the alignment procedure, each alignment constant is controlled: 'penalty-terms' are added to the $\chi^2$ to minimize. These extra-terms prevent the variation of the alignment parameters (w.r.t. the initial survey value) to be significantly larger than the metrology precision.

The results of applying this second step of the alignment procedure to simulation events are given in section 4.2.

### *3.3 Detector-halves Alignment*

The final step of the alignment procedure is to perform the relative alignment of the two detector-halves. Clearly, the module space-point residuals within a detector-half are not sensitive to the misalignment of the whole half. Thus, observables connecting the two detector-halves have to be used.

Tracks that pass through both VELO detector-halves, referred to here as over-

lap tracks, provide a powerful constraint for the relative positioning of the two detector-halves. These tracks are required to have at least one space-point (*i.e.* an $(r, \phi)$ cluster pair) in each VELO detector-half. The VELO was specifically designed to obtain such a class of tracks: the modules from the VELO left and right-halves are offset in z and interlace by a small distance when closed. The overlapping area between the two VELO detector- halves, when fully inserted, corresponds to 2% of the active surface area of the sensors.

Having selected these overlap tracks, the alignment proceeds by residual minimization using the same technique as the module alignment. An equivalent of Eqn. 2 is thus required in terms of the relative alignment constants of the two detector-halves. Assuming that the alignment of the modules in each detector-half has been already corrected, then the equation for the residuals becomes (see Ref. (8)):

$$\begin{cases} \epsilon_{\mathrm{x}} = -\Delta^B_{\mathrm{x}} + \mathrm{z}^B_0 \cdot \Delta^B_\beta + \mathrm{y} \cdot \Delta^B_\gamma + a \cdot (\Delta^B_{\mathrm{z}} + \mathrm{x} \cdot \Delta^B_\beta + \mathrm{y} \cdot \Delta^B_\alpha) \\ \epsilon_{\mathrm{y}} = -\Delta^B_{\mathrm{y}} + \mathrm{z}^B_0 \cdot \Delta^B_\alpha - \mathrm{x} \cdot \Delta^B_\gamma + c \cdot (\Delta^B_{\mathrm{z}} + \mathrm{x} \cdot \Delta^B_\beta + \mathrm{y} \cdot \Delta^B_\alpha) \end{cases},$$

where $\Delta^B_{\mathrm{x}},\ \Delta^B_{\mathrm{y}},\ \Delta^B_{\mathrm{z}},\ \Delta^B_\alpha,\ \Delta^B_\beta,\ \Delta^B_\gamma$ are the detector-half degrees of freedom (position of one half with respect to the other), and $\mathrm{z}^B_0$ the z position in the detector-half frame of the module in which the space-point hit was recorded.

The matrix inversion technique then allows these six relative alignment constants of the detector-halves to be determined, assuming the VELO is fully inserted for physics data taking.

However, during insertion and during the commissioning phase an alignment may be required with the VELO in the retracted position. In this case the rate of overlap tracks becomes very small and an alternative technique is required. The detector-half alignment can then be performed using vertices as constraints. Tracks from the primary interaction point can be used if available or beam-gas interactions occurring in the VELO vacuum tank. By fitting for the vertex separately inside each of the two detector-halves, one can obtain the misalignment between the two halves.

Assuming that one box is fixed (*i.e.* using it to define the co- ordinate system) the reference vertex position can be determined from this half. The vertex position found using the tracks passing through the other detector-half is related to the misalignment between the two halves via the following relations:

$$\begin{cases} v^B_{\mathrm{x}} = b_i + a_i \cdot v^B_{\mathrm{z}} + \Delta^B_{\mathrm{x}} - a_i \cdot \Delta^B_{\mathrm{z}} - v^B_{\mathrm{z}} \cdot \Delta^B_\beta \\ v^B_{\mathrm{y}} = d_i + c_i \cdot v^B_{\mathrm{z}} + \Delta^B_{\mathrm{y}} - c_i \cdot \Delta^B_{\mathrm{z}} - v^B_{\mathrm{z}} \cdot \Delta^B_\alpha \end{cases},$$

where $a_i, b_i, c_i, d_i$ are the parameters of the $i^{th}$ track used to fit the vertex,

$(v_{\mathrm{x}}^B, v_{\mathrm{y}}^B, v_{\mathrm{z}}^B)$ the vertex position in the 'moving' half, and $\Delta_i^B$ denote the detector-half degrees of freedom (position of one half with respect to the other). It is easy to relate this formulation to the residual formalism used previously. Indeed, the residual in this case will be the differences between the vertices positions fitted within the two halves:

$$\begin{cases} v_{\mathrm{x}}^B = v_{\mathrm{x}}^{ref} + \epsilon_{v_{\mathrm{x}}} \\ v_{\mathrm{y}}^B = v_{\mathrm{y}}^{ref} + \epsilon_{v_{\mathrm{y}}} \\ v_{\mathrm{z}}^B = v_{\mathrm{z}}^{ref} + \epsilon_{v_{\mathrm{z}}} \end{cases} .$$

where $(v_{\mathrm{x}}^{ref}, v_{\mathrm{y}}^{ref}, v_{\mathrm{z}}^{ref})$ defines the vertex position in the fixed half, *i.e.* the reference value.

Having determined these relations, the same technique can again be used to determine the alignment constants: even though we are now using vertices rather than track residuals the Millepede framework is still applicable as it does not depend on the object that is being fitted.

More details on this novel technique of alignment with vertices can be found in Ref. (8). The vertex fitting method can also be used to determine the VELO detector-halves' positions with respect to the beam, when using vertices from the primary interaction point.

The results of applying this final step of the alignment procedure to simulation events are given in section 4.3.

## 4 Simulation Studies

A simulation of 200 samples of 25,000 events each has been produced and propagated through the LHCb software. Each sample, which comprises a mixture of 5,000 minimum bias events ($\approx$ 100,000 tracks from primary vertex interactions) plus 20,000 beam-halo like events, was produced with a different set of alignment constants. The misalignment values have been randomly chosen within a Gaussian distribution centered on zero and with resolutions based on construction and survey accuracies (defined in Ref. (8)). All the module and detector-half degrees of freedom have been misaligned. The initial step, the relative sensor alignment, was tested using different event samples which are described in the first part of this section.

The sensor alignment method has been tested with 10 samples of randomly generated misalignments. All sensors have been misaligned individually, thus generating a scenario equivalent to simultaneous module to module and sensor to sensor misalignments. Each of the 10 samples consists of 20,000 tracks with small slopes, thus passing through all sensors of one VELO-half and evenly distributed across the sensor surface. Typically three iterations of the alignment procedure are required to obtain the best resolution.

Fig. 4 shows the generated and the remaining misalignments after all iterations. The resolution on the relative x and y translation of the sensors of one module is 1.3 $\mu$m, *i.e.* a significant improvement over the survey precision. The performance of this algorithm has also been demonstrated with beam test data and is reported in Ref. (2).

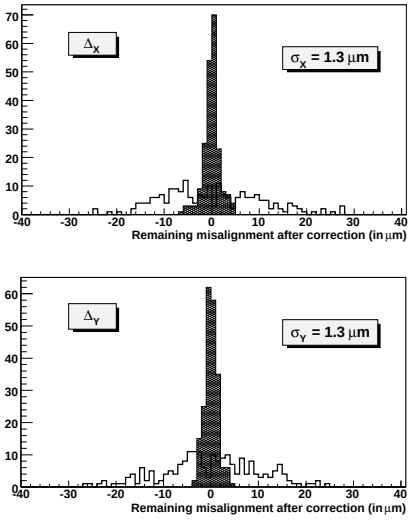


Fig. 4. Misalignment values before (□), and after (■) sensor relative alignment.

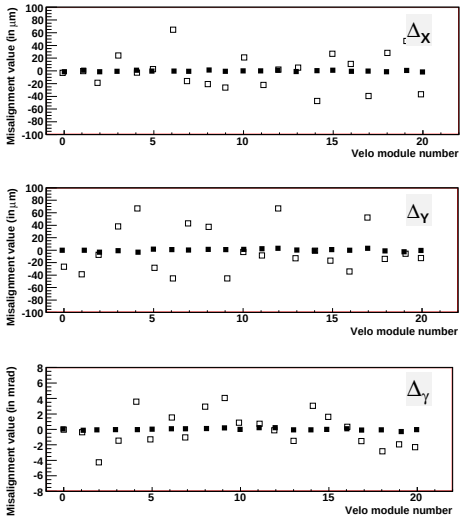


Fig. 5. Misalignment values in one detector-half before (□), and after (■) internal alignment.

*4.2 Relative Module Alignment Results*

The internal alignment of the modules in each detector-half is primarily sensitive to translations of the modules in the X and Y directions and rotations around the Z-axis. Results on the alignment of all modules in a detector-half, for one particular sample, are presented in Fig. 5. In Fig. 6 the alignment constants for 200 event samples, before and after correction, are shown. Resolutions on the X and Y translation alignment parameters of 1.1 $\mu$m and on rotations around the $z$-axis of 0.12 mrad are obtained. About 20,000 tracks per

detector-half were needed to obtain this accuracy. The alignment resolutions are well below the intrinsic detector hit resolution. The performance of this algorithm has also been demonstrated with beam test data and is reported in Ref. (2).

Concerning the 'non-linear' degrees of freedom, the observed sensitivity is as expected worse than for the other parameters. However some results were obtained for the modules which are close to the interaction region, *i.e.* where track slopes are larger. Restricting the study to these stations (1 to 14), one obtains a reasonable sensitivity to $\Delta_z$ (28 $\mu$m) and a fair sensitivity to $\Delta_\alpha$ and $\Delta_\beta$ (0.8 mrad and 1.1 mrad respectively). This sensitivity is worse than the survey precision, but will provide a cross-check of this survey information.

As this algorithm is in general run independently of the relative sensor alignment algorithms its performance has been evaluated separately. In the presence of relative misalignments of the sensors on a given module the module's position will be aligned to the average position of the two sensors [2].

### *4.3 Detector-halves Alignment Results*

Although the three alignment steps can be performed independently, in practice it is expected that steps two and three will be run consecutively. Hence, the results presented in this section are for the realistic case of performing both of these alignment steps on misaligned samples. The tracks are refitted after the module alignment procedure in order to update the track parameters. The results presented here have been obtained with about 300 overlap tracks.

The results of the study are presented on Fig. 7. The resolution on the X and Y translation alignment parameters is 12 $\mu$m for x and y translations, and the resolution on the x and y tilts is 36 $\mu$rad.

As in the case of the module alignment, some of the degrees of freedom are more difficult to constrain. In the detector-half alignment these weakly constrained motions are the ones related to the Z-axis: rotation around and translation along. The relative rotation around Z between the two detector-halves is constrained using the overlap tracks. Translations along Z are estimated through the vertex fitting technique. The vertices are fitted separately from tracks in each detector-half and the misalignment determined by comparing the Z positions, from this a 40 $\mu$m resolution was obtained.

[2] This requires a track sample with a sufficiently flat distribution in $\phi$ which is given for the samples used for VELO alignment.

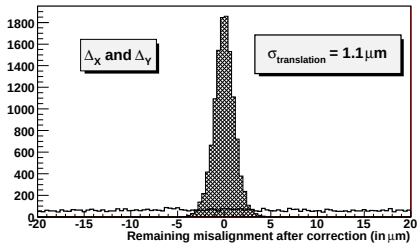


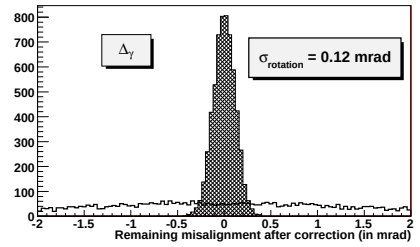


Fig. 6. Misalignment values before (□), and after (■) internal alignment, for all configurations and all stations.

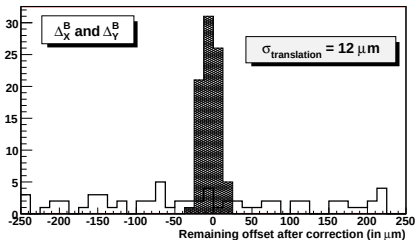


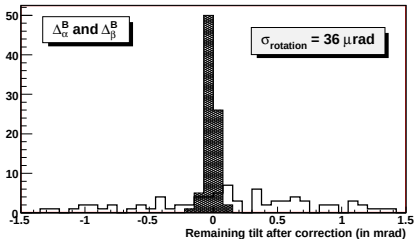


Fig. 7. Misalignment values before (□), and after (■) detector halves alignment, for all configurations.

## 5 Conclusion

A software alignment method for the LHCb vertex locator has been developed. This procedure performs the alignment in three steps, all using track residuals. First, a relative alignment of the $R$ and $\Phi$ sensors within each VELO module is performed. This is followed by an internal alignment of the VELO modules within each detector- half. Thirdly, since the detector-halves are moved between each LHC fill, a final step is required in order to align the detector-halves with respect to each other, thus providing a fully internally aligned VELO.

Due to the VELO module design ($R$ and $\Phi$ sensors are glued onto the same hybrid and precisely surveyed), it is foreseen to perform the first stage with a much lower frequency than the two other ones and to use it for the annual data reprocessing. The alignment of the relative sensor position achieves a precision of 1.3 $\mu$m for x and y translations.

The final two stages of VELO alignment strategy use the Millepede program, which enables the alignment to be performed in only one pass; this is to be compared with classic minimization methods which require many iterations to provide their result. This technique allows the processing of module and VELO-half alignment within a few minutes on a single CPU [3], assuming that an appropriate data sample is available.

[3] 1 CPU = 1000 SpecInt2000 units

For the internal alignment of the modules in a detector-half a 1.1 $\mu$m precision has been achieved on the relevant translational degrees of freedom (*i.e.* along X and Y axes), and a 0.1 mrad accuracy on the rotation around the Z-axis. These values are well below the expected detector intrinsic resolution. Future work will be undertaken to enable an efficient selection of the required tracks in the LHCb trigger.

The results of the detector-half alignment procedure show that the tracks that pass through the overlap region between the two VELO detector-halves provide a very strong constraint. With only a few hundred tracks accuracies of 12 $\mu$m for x and y translations, and 36 $\mu$rad for X and Y tilts, are obtained. These results are well within the system requirements.

This paper has described the algorithms developed to perform the alignment of the LHCb VELO and demonstrated with simulation samples that this approach provides the performance required so that misalignment effects will not adversely affect the LHCb physics programme.

## References


[1] *CERN-2007-004* (2007).
[2] S. Viret *et al*, *submitted to NIM* (2007).
[3] LHCb Collaboration, *CERN-LHCC 2003-030* (2003).
[4] LHCb Collaboration, *CERN-LHCC-2002-029* (2002).
[5] D. Petrie, C. Parkes, S. Viret, *LHCb 2005-059* (2005).
[6] M. Gersabeck, S. Viret, C. Parkes, *LHCb 2007-138* (2007).
[7] S. Viret, C. Parkes, D. Petrie, *LHCb 2005-101* (2005).
[8] S. Viret, C. Parkes, M. Gersabeck, *LHCb 2007-067* (2007).
[9] C.D. Jackson, D. Su, F.J. Wickens, *CERN-2007-004* (2007) 59–70.
[10] V. Blobel, *CERN-2007-004* (2007) 5–12.
[11] C. Kleinwort, *CERN-2007-004* (2007) 41–50.
[12] R. Mankel, *CERN-2007-004* (2007) 51–58.
[13] T. Lastovicka, *LHCb-2007-002* (2007).